minerals

MDPI

Article

Strength Performance and Microstructures of Alkali-Activated Metakaolin and GGBFS-Based Mortars: Role of Waste Red Brick Powder Incorporation

Hussam Alghamdi *, Aref A. Abadel *, Mohammad Khawaji, Mohammed Alamri and Abdullah Alabdulkarim

Department of Civil Engineering, College of Engineering, King Saud University, Riyadh 12372, Saudi Arabia; mkhawaji@ksu.edu.sa (M.K.); mohdalamri@ksu.edu.sa (M.A.); alabdulkarim@ksu.edu.sa (A.A.)
* Correspondence: hsghamdi@ksu.edu.sa (H.A.); aabadel@ksu.edu.sa (A.A.A.)

Abstract: Excessive use of natural resources and environmental concerns are key issues motivating the recycling of waste materials in the construction industry to minimize landfill problems. Free cement binders such alkali-activated binders have emerged as a prospective alternative to ordinary Portland cement, wherein diverse industrial, agriculture, and by-product waste materials have been converted as valuable spin-offs. Annually, tens of millions tons of red brick wastes are generated, which leads to several environmental problems. Thus, waste red brick powder (WRBP) was used as binder or a fine aggregate (silica sand) substitute to prepare some new types of alkali-activated mortars (AAMs). These mortars contained ground blast furnace slag (GGBFS) and metakaolin (MK) with various levels of WRBP (0, 15, 30, and 45%) as a substitute for silica sand. The prepared AAMs were cured at 300 °C, 600 °C, and ambient temperature. All the specimens were tested to determine the effects of various WRBP contents on the workability, strengths, and microstructures of the designed AAMs. The workability of the fresh AAMs was considerably dropped due to the incorporation of WRBP as binary binder or fine aggregate replacement. In addition, AAM containing 15% of WRBP as GGBFS and MK replacement displayed a significant improvement (by 30.7%) in the strength performance. However, the increasing content of WRBP to 30% and 45% significantly led to a decrease in compressive strength from 49.9 MPa to 44.7 and 34.2 MPa, respectively. Overall, the mortars' strength was increased with the increase in WRBP contents from 0 to 45% as sand substitute. Conversely, the mortars strength was reduced with the increase in curing temperatures. The microstructure analyses of the studied mortars revealed an appreciable enhancement of the geopolymerization process, gels formulation, and surface morphology, leading to an improvement in their compressive and flexural strength characteristics. It was asserted that high-performance mortars with customized engineering properties can be designed via the inclusion of WRBP into alkali-activated MK-GGBFS mixes.

Keywords: alkali-activated mortars; waste red brick powder; slag; metakaolin; workability; curing regimes; strength performance; microstructure

Citation: Alghamdi, H.; Abadel, A.A.; Khawaji, M.; Alamri, M.; Alabdulkarim, A. Strength Performance and Microstructures of Alkali-Activated Metakaolin and GGBFS-Based Mortars: Role of Waste Red Brick Powder Incorporation. *Minerals* **2023**, *13*, 848. https://doi.org/10.3390/min13070848

Academic Editors: Jie Ren, Linfei Li and Zhenhua Wei

Received: 14 May 2023
Revised: 15 June 2023
Accepted: 20 June 2023
Published: 23 June 2023

1. Introduction

Since its emergence, ordinary Portland cement (OPC) remains the foremost binder for concrete production. Over the years, the demand for OPC in developed countries has significantly increased despite its negative impact on the environment. Not only does the production process of OPC consume high energy, but it also causes high carbon dioxide (CO_2) emissions [1,2]. In short, OPC is an environmentally hazardous binder as the emission of greenhouse gas like CO_2 during its manufacturing has severe impact on climate change [3]. These factors drove scientists and engineers worldwide to explore some versatile binder alternatives to OPC [4]. The main idea is to develop some novel

environmentally friendly binders like green mortars or concrete using recycled wastes dumped as landfill that cause another burden to environment [5].

Presently, various cement-free binders have been introduced as environmental remedies wherein the CO_2 emission from these green binders is low [6–8]. In addition, these new binders are preferred over OPC due to their lower energy consumption in the production process, less landfill-related issues, reduced usage of natural resources, lower cost, and lower total demand in construction industries [9–11]. Usually, cement-free binders with alkali solution activation are produced by mixing various by-products and agricultural wastes that are enriched in calcium, magnesium, and aluminosilicate oxides (Al_2O_3-SiO_2) [12–14]. Over the decades, numerous types of industrial, agriculture, and by-product waste materials such as fly ash, palm oil fuel ash, ceramic tiles, bottom ash, and ground blast furnace slag and metakaolin have successfully been used to produce high-performance cement-free concrete and mortars [15,16]. Consequently, it has been established that green binders/mortars made from diverse industrial and agricultural wastes via the alkali solution activation can potentially contribute towards sustainable development, wherein these AAMs can lower the level of CO_2 emission as much as 75% more than conventional OPC [17]. Despite many efforts, a high-performance OPC-free alkali-activated binder made from various waste materials still has not been determined.

Waste red bricks (WRBs) that are mainly obtained from bulldozed buildings constitute a large portion of destroyed construction components [18,19]. It was reported that demolished wastes from the construction sectors worldwide presents about 20%–60% of total solid waste, contributing about 10 billion tons of waste per year [20]. WRB powder (WRBP), being a pozzolanic material, has many notable attributes like dominant amorphous phases, particles size distribution, specific surface areas, and so forth that are effective for sustainable cement-free construction materials production [5]. In recent years, a significant amount of WRBs has been used as the coarse aggregates in roadway landscapes and manufacturing of structural as well as non-structural mortars/concretes [21]. Repeated studies have revealed that WRBP can successfully be used as a precursor in cement-free materials including geopolymer and alkali-activated mortars/binders [22]. As aforementioned, WRBP is enriched in Al_2O_3-SiO_2 with interesting engineering attributes and can produce excellent binders when activated using alkali solutions. Diverse industrial wastes and spin-offs utilized in the construction sectors are known for their environmental friendliness, and thus the frequently used precursors (FA, POFA, GGBFS, and others) contain high volume of amorphous silica and/or Al_2O_3-SiO_2 [23]. The other precursor used for geopolymer mortars fabrication is MK obtained from the calcination process (at 750 °C) of rocks that contain kaolinite [24,25]. However, the manufacturing of MK is very costly, energy-intensive, and has adverse environmental impacts. In this view, WRBP can be a potential alternative to MK for the production of cement-free AAMs or alkali-activate binders.

Ma et al. [26] studied the effect of WRBP on the engineering properties of cement composites such as water absorption, pozzolanic activity, and compressive strength. The pozzolanic action of WRBP was shown to increase with increasing fineness. In addition, it was concluded that the inclusion of WRBP with suitable fineness can reduce the porosity and water absorption features of the composites, enhancing its strength and workability. Meanwhile, the advantage of activating mortars by alkaline solution was demonstrated in converting WRBP into greener cement [27,28]. The cement-free binders were designed using WRBP to examine their environmental benefit wherein the AAMs displayed analogous performance to conventional cement [29]. The environmental benefits of AAM were more significant compared to OPC; the energy utilization and emission of greenhouse gases were 45% and 72% lower compared to OPC, respectively. The binary cement-free binders using WRBP (at various contents) as a partial precursor were made to evaluate the effects of substitution level on the mortars' strength properties [30]. The WRBP-GGBFS binder showed optimum strength characteristics. In comparison to the applications of WRBP in the cement industry, its uses in the alkali-activated materials are inadequate and not fully

formed. Thus, some extensive studies are needed to determine the potential uses of WRBP in the design of alkali-activated mortars or binders.

Based on abovementioned literature overview, the main aim of this study is to develop high-performance AAMs using WRBP-based binder and filler. The binary blends (GGBFS and MK) and fine aggregates (silica sand) were replaced by various amounts of WRBP to make a new type of AAMs and tested thoroughly. The effect of WRBP contents on the workability, bulk density, compressive, flexural strength, efflorescence, and visual appearance of the AAMs are evaluated. The obtained AAMs were examined using X-ray diffraction (XRD) and scanning electronic microscopy (SEM) analysis to determine the effect of various WRBP contents on their microstructures and surface morphology.

2. Experimental Procedures

2.1. Raw Materials and Mixtures Proportioning

In this work, raw materials like MK and GGBFS were utilized as main source to synthesize the proposed AAMs wherein the WRBP was used as binder and fine aggregates replacement. WRBP was locally collected and ground using a Los Angeles grinder machine. The commercial MK and GGBFS were used in this experimental as received from the supplier. The chemical composition of utilized materials including MK, GGBFS, and WRBP were evaluated using an X-ray fluorescence spectroscopy (XRF) test (Rigaku NEX-CG EDXRF). Table 1 shows the chemical compositions of MK, GGBFS, and WRBP which were mainly composed of CaO, Al_2O_3, and SiO_2. For the MK and WRBP, the primary oxides were found to be SiO_2 and Al_2O_3 which are 93.62% in MK and 81.35% in WRBP. Contrarily, the main elements in GGBFS were found to be CaO, SiO_2, and Al_2O_3 (96.15%). The highest content of CaO was found in GGBFS (37.67%) compared to low content in MK (1.28%) and WRBP (6.15%). The utilized materials' particle sizes were obtained using a particle size analyser test (Mastersizer 3000). Figure 1 displays the particle size distribution of MK, GGBFS, and WRBP. From the obtained results, it was found that the median particles size of MK, GGBFS, and WRBP are 32.3, 9.7, and 223 μm, respectively.

Table 1. Chemical compositions of the raw source materials.

Composition	MK	GGBFS	WRBP
CaO	1.287	37.679	6.15
SiO_2	50.995	41.633	66.55
Al_2O_3	42.631	16.857	14.80
Fe_2O_3	2.114	0.144	5.48
SO_3	0.439	1.833	--
MgO	0.127	1.184	2.39
K_2O	0.337	0.360	2.13
Na_2O	0.284	0.216	--
ZnO	0.004	0.000	--
LOI	--	--	1.48

The X-ray diffraction (XRD) patterns of MK, GGBFS, and WRBP were obtained using the X-ray diffraction test. Figure 2 displays the XRD profiles of MK, GGBFS, and WRBP indicating their amorphous nature in the presence of a broad hunch at 2θ = 20–30° (for MK), 25–35° (for GGBFS), and 15–30° (for WRBP). The glassy nature of these resources enabled their strong reactivity during the geopolymerization process. The XRD patterns of MK and WRBP showed intense crystalline peaks, confirming the existence of quartz.

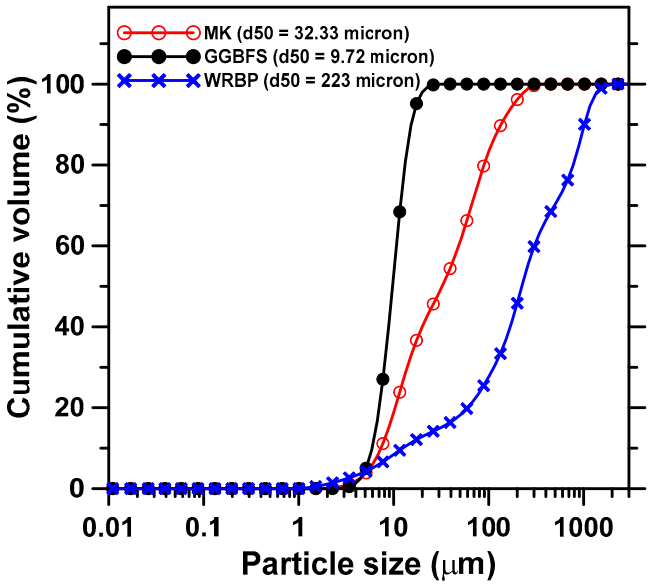

Figure 1. Particle Size Distribution (PSD) of MK, GGBFS, and WRBP.

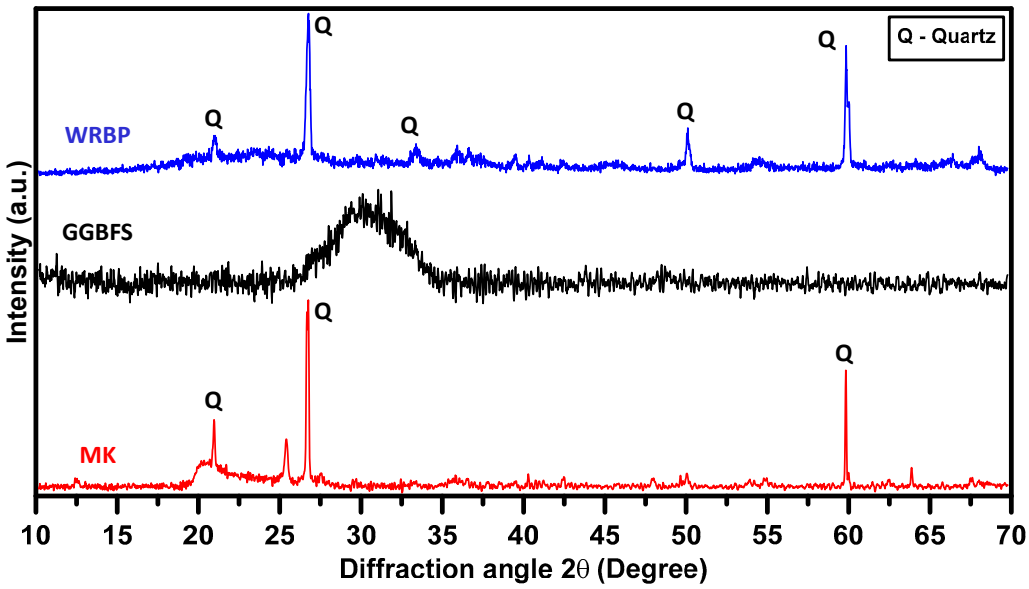

Figure 2. XRD profiles of MK, GGBFS, and WRBP.

The solutions of sodium silicate (supplied by Golden Shell Corporation with solid contents of 37.43%, silica modulus, M_s = 3.41, and specific gravity of 1.38 g/cm^3) and sodium hydroxide (NaOH) were used as alkali activators for the design of mortars. First, sodium silicate solution was added with NaOH to lower the value of M_s and desired Na_2O to total powder (n). For sample preparations, two major parameters—N_2O-binder ratio (n) and the silica modulus (M_s = molar ratio of SiO_2 to N_2O)—were followed to proportion the activator solution. According to the previous studies [31–33], the optimum (n) and (M_s) values for MK and GGBFS were 0.12 and 1.8, respectively, to avoid carbonation and leaching issues due to increasing alkalis in the systems and also achieve better mechanical properties. The water-to-binder ratio (mass based) used to prepare the mixtures was 0.5 to ensure sufficient workability for alkali-activated MK-GGBFS systems. The WRBP content ranged from 0% to 45% with an increment step of 15%. Fine aggregates (silica sand) following ASTM C33 [34] were added to the mixtures with volume fraction of 50% to prepare mortars. Two scenarios were adopted in this study; first, WRBP was used as replacement by MK and GGBFS, and the second scenario was that WRBP was used as a replacement by silica

sand. In preparing the proposed mortar' specimens, Table 2 shows the composition of all mixture proportions. The preparation of the proposed mortars' mixing of ternary binders included MK, GGBFS, and WRBP for the duration of 180 s resulting in a uniform dry substance, which was then further mixed with silica sand for a period of 240 s. Then, the two-part alkaline activator solution (sodium hydroxide and sodium silicate) was added to the mixture, then blended in a machine for a further 300 s at medium velocity. Finally, the resulting mortar was introduced into the moulds which was achieved by using the two-layers pouring method, each layer being subject to the vibration table for 20 s to allow the escape of air voids. In this process, each layer was subject to vibration for a period of 15 s in order to eliminate any air pockets within the mixture. All mortar specimens were cast and left in the mould at ambient temperature for 24 h and then demoulded and stored in a humid chamber (23 ± 1 °C, 30% RH) for 28 days. For the purpose of investigating the thermal stability and fire resistance properties of the prepared mortar samples, the samples were cured and exposed for 3 h to two different high temperatures (300 °C and 600 °C).

Table 2. Mix proportions of AAMs containing WRBP as binder and fine aggregate substitute.

Scenarios	Sample ID	GGBFS (g)	MK (g)	WRBP (g)	Sodium Silicate (g)	NaOH (g)	Water (g)	Sand (g)
WRBP used as replacement (MK+GGBFS)	SM_Control	500	500	0	729.0	73.0	192	2705
	SMRC15	425	425	150	729.0	73.0	192	2705
	SMRC30	350	350	300	729.0	73.0	192	2705
	SMRC45	275	275	450	729.0	73.0	192	2705
WRBP used as replacement by silica sand	SM_Control	500	500	0	729.0	73.0	192	2705
	SMRS15	500	500	406	729.0	73.0	192	2299
	SMRS30	500	500	812	729.0	73.0	192	1894
	SMRS45	500	500	1217	729.0	73.0	192	1488

2.2. Test Methods

Mortar mixtures were prepared based on the proportions as shown in Table 2 to investigate the workability behaviour of designed mortars with various levels of WRBP as binder and fine aggregate replacement. The flow table tests were conducted according to ASTM C230 [35] using a flow table machine to understand the role of WRBP addition on the fresh properties of AAMs. In addition, the effect of WRBP on the bulk density of the prepared mortars was evaluated. In line with ASTM C109 [36] and ASTM C78 [37], the prepared mortars were tested for their compressive and flexural strength at 28 days of curing age using a compression machine (3000 kN capacity NL Scientific). Specimens with size of 50 × 50 × 50 mm were casted and considered for the compressive strength test. A constant rate (2.5 KN/s) of loading was selected and applied to the failure of the specimen. Since the machine has inbuilt configurations, the density and compressive strength are generated automatically based on the imputed specimen weight and dimensions. For the flexural strength test, prism specimens with size of 40 × 40 × 160 mm were used and the three-point test was carried out using the universal testing machine. The obtained results of the proposed AAMs were compared with the one made without WRBP (control sample) and the final values were recorded using averaging of the three samples. To conduct the microstructure test including XRD and SEM, the AAMs was found to collapse after 28 days. The central part of each collapse sample after 28 days was removed and pulverized as fine powders for additional tests. XRD data (2θ = 10–70°, step size of 0.02° and scan (Rigaku, Tokyo, Japan) speed of 0.5 s/step) were analysed using Jade software, confirming the amorphous phase of the prepared AAMs. The AAMs after the compressive strength test at 28 days was obtained for the SEM analysis wherein each specimen was placed onto double cellophane papers and then glued on the coin before being coated by the gold sputter coating instrument. Then, the scanning electronic machine (Jeol, JSM-IT300, Tokyo, Japan) was used to evaluate the surface morphology of selected specimens.

3. Results and Discussion

3.1. Workability Performance

Figure 3 illustrates the effect of different WRBP contents (15, 30, and 45%) as MK and GGBFS replacement on the workability of the designed AAMs. The workability performance of the AAMs was negatively affected by the variation of WRBP contents. The mixture containing 45% of WRBP displayed the lower flow (120%) compared to the control sample (130%). The reduction in flowability of the high amount of replacement was attributed to the high porosity of WRBP, which resulted in an increment on water demand. It is well known that the high demand of water in the mixture negatively affects its workability performance. WRBP has a relatively higher inter-particle friction and, as a result, a reduction in flow is expected [38].

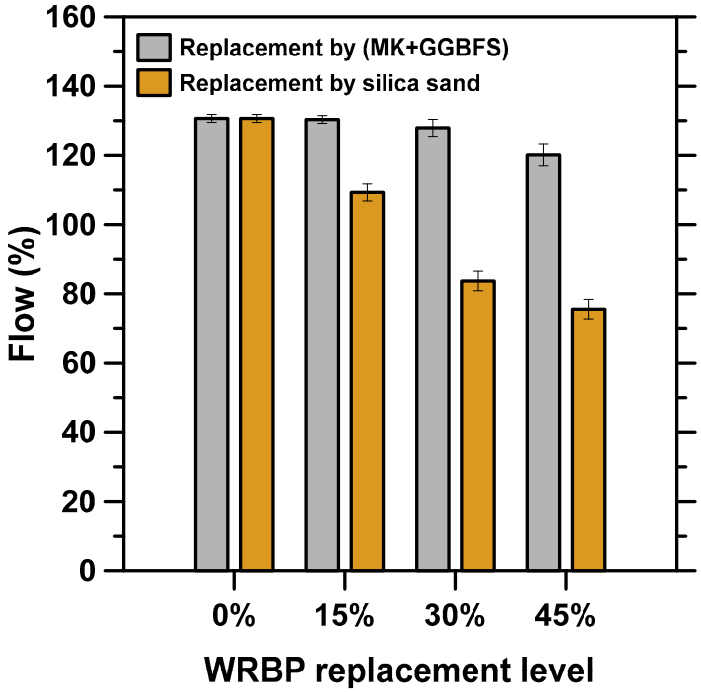

Figure 3. Effect of WRBP replacement type (scenario) on flowability of mortar samples.

The effect of WRBP as a silica sand replacement on the prepared mortars' workability was evaluated and the obtained results are presented in Figure 3. Silica sand was replaced by 15, 30, and 45% of WRBP. The results revealed that the increasing replacement level of silica sand by WRBP from 0 to 45% led to a drop in the flow from 130% to 75%, respectively. It is well known that a high demand of water by WRBP compared to silica sand can significantly affect the workability performance of the mortars, producing lower flow readings compared to the control sample. Huseien et al. [39] observed that the workability of alkali-activated materials can significantly be influenced by the fineness of sand, whereas when increasing the fineness, the flowability of mortars tend to decrease.

The results showed that the mixtures prepared with WRBP as silica sand replacement achieved lower workability compared to those mixes made with WRBP as MK and GGBFS replacement. However, in both cases the increasing level of WRBP up to 45% significantly affected the workability performance of the AAMs. The lower flow change (75%) of the mixture containing 45% of WRBP as silica sand replacement than the one made with WRBP as MK and GGBFS replacement (120%) was attributed to the high amount of WRBP (1217 g) compared to 450 g. The high volume of WRBP in the AAMs led to an increase in the water demand and loss of workability.

3.2. Mechanical Properties

3.2.1. Effect of WRBP on Bulk Density

Table 3 presents the bulk density of the studies AAMs as a function of WRBP contents. For the specimens prepared with WRBP as GGBFS and MK replacement and cured at ambient temperatures, the increasing content of WRBP from 0 to 30%, led to an increase in the bulk density from 2.263 to 2.399 g/cm^3. However, the increasing WRBP content to 45% resulted in the bulk density dropping to 2.340 g/cm^3. Compared to ambient temperature curing, all the alkali-activated curing at the elevated curing temperatures of 300 and 600 °C displayed lower bulk density. However, the specimens containing 45% of WRBP shown more stable bulk density under different curing temperatures. For the specimens prepared with WRBP as silica sand replacement, the inclusion of 30 and 45% of WRBP caused a drop in the bulk density compared to the control sample for all different curing regimes. The change in the density of the prepared specimens as significantly influenced by the specific gravity of WRBP compared to MK, GGBFS, and silica sand.

Table 3. Bulk density of mortars cured at different temperatures.

Sample ID	Bulk Density (g/cm^3) of Cured Specimens		
	At Ambient Temp. for 28 days	At 300 °C for 3 h	At 600 °C for 3 h
SM control	2.263 (0.006)	2.206 (0.007)	2.209 (0.010)
SMRC15	2.291 (0.006)	2.203 (0.007)	2.208 (0.010)
SMRC30	2.399 (0.008)	2.145 (0.008)	2.239 (0.009)
SMRC45	2.340 (0.008)	2.309 (0.010)	2.286 (0.007)
SM control	2.263 (0.006)	2.206 (0.009)	2.209 (0.010)
SMRS15	2.272 (0.009)	2.227 (0.009)	2.243 (0.009)
SMRS30	2.241 (0.009)	2.175 (0.006)	2.201 (0.006)
SMRS45	2.204 (0.009)	2.161 (0.008)	2.188 (0.007)

3.2.2. Effect of WRBP Content on Compressive Strength

Figure 4 illustrates the compressive strength of the AAMs prepared using WRBP as GGBFS and MK replacement at 28 days of curing age. The inclusion of WRBP as ternary binder replacement was shown to significantly improve the compressive strength. The replacement of MK and GGBFS by 15% of WRBP led to a remarkable improvement in the geopolymerization process, increasing the compressive strength from 37.54–49.98 MPa. On the other hand, the increasing replacement level of MK and GGBFS by WRBP from 15 to 45% led to a drop in the compressive strength from 49.98 to 34.20 MPa, respectively. It is well known that the calcium and aluminium oxides significantly affect the alkali-activated materials' strength development [40]. With dropping levels of MK and GGBFS from a 100% based binder to 70% and 55%, the content of both oxides significantly decreased and affected the dense gels formulation; this reduction in gel formulation eventually led to an increase in the pores, thereby causing lower strength. Additionally, since silicon oxide cannot exist in its free form at the temperatures required to produce red bricks, and since the WRBP lacks free significant amorphous content (Figure 2), this decrease in compressive strength can be attributed to the effect of higher WRBP content in the mixtures proportioned using 30% and 45% WRBP and the alkalinity of the activator might not be high enough to enable the formation of a sufficient amount of reaction products by breaking down the Si–O–Si and Al–O–Al bonds. In addition to this, the compressive strength of the suggested AAMs was affected by the large particle sizes of the WRBP in comparison to those of the MK and GGBFS, which led to a lower strength in comparison to the control specimen.

Earlier studies indicated the effects of quartz powder towards improvements in the strength of mortars [41,42]. In the present work, the obtained reduction in the gel formulation was mainly due to the participation of quartz as extra nucleation sites for the reaction product which could restrict the distortion of the mortar's matrix via the mechanical constraints. This in turn ensured the generation of strong interfacial transition zones

amid the particles of quartz and the alkali-activated pastes. In addition, the strong reaction among aluminosilicate particles and feldspars present in WRBP with the alkali solution produced various reaction products with strong binding traits. The observed increase in the mechanical strength of the AAMs can be ascribed to the existence of amorphous silica that were generated from the calcium-silicate hydrates [43].

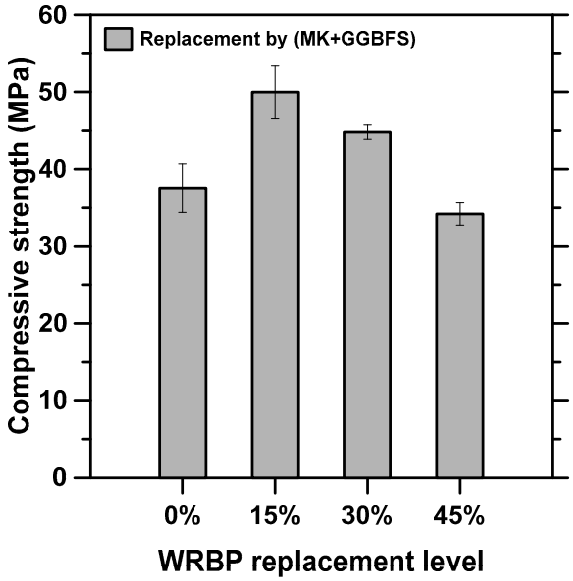

Figure 4. Compressive strength of AAMs as a function of WRBP contents as MK+GGBFS replacement.

Figure 5 displays the variation of flexural strength of the designed AAMs as a function of WRBP contents as MK+GGBFS replacement at 28 days of curing age. The replacement of the ternary binder by 15% of WRBP led to an improvement in the flexural strength from 4.88 to 5.64 MPa. However, the increasing content of WRBP to 30 and 45% caused a drop in flexural strength values to 5.23 and 2.29 MPa, respectively. The high content of WRBP (30 and 45%) in AAMs caused a drop in the content of CaO and Al_2O_3 and reduced the total dense gels formulation.

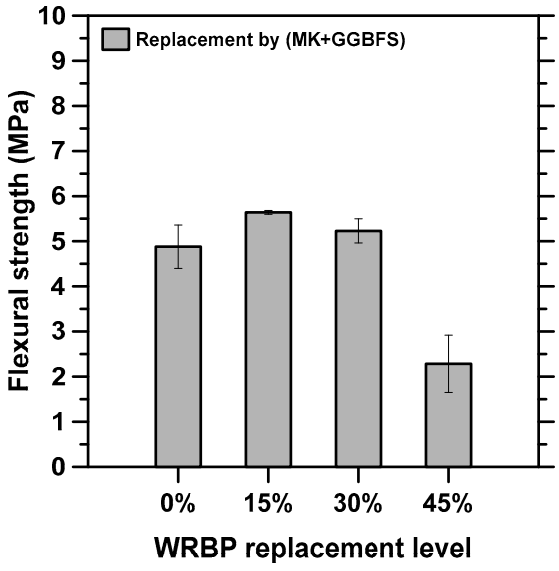

Figure 5. Effect of WRBP replacement (%) for MK+GGBFS on the flexural strength of AAMs.

Figure 6 illustrates the effect of WRBP as silica sand replacement on strength development of the prepared mortars at 28 days of curing age. The results indicated that the

increasing level of replacement of WRBP from 0 to 45% significantly enhance the gained compressive strength. The compressive strength was increased from 37.54 to 89.62 MPa with a raising level of WRBP from 0 to 45%, respectively. Likewise, the inclusion of WRBP in the mortars matrix as silica sand replacement was found to improve the flexural strength values (Figure 7). Compared to the control sample, all the specimens containing various levels of WRBP achieved higher flexural strength values. Specimens prepared with 15% of WRBP displayed flexural strength 6.10 MPa compared to the control sample (4.88 MPa). The specimens prepared with 30 and 45% achieved almost similar flexural strength of 6.20 and 6.30 MPa, respectively.

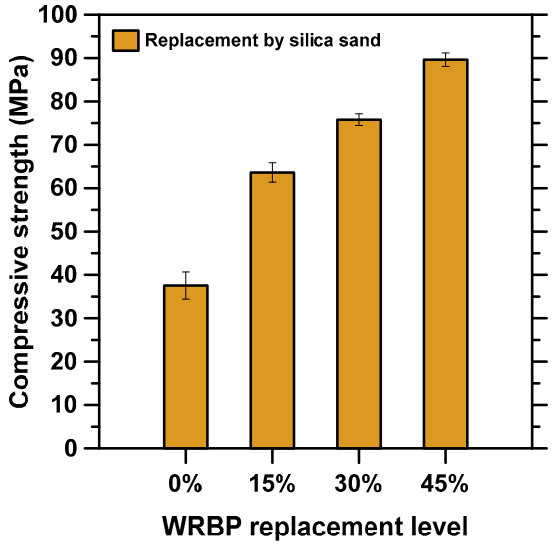

Figure 6. CS of AAMs against varying WRBP contents as silica sand replacement agent.

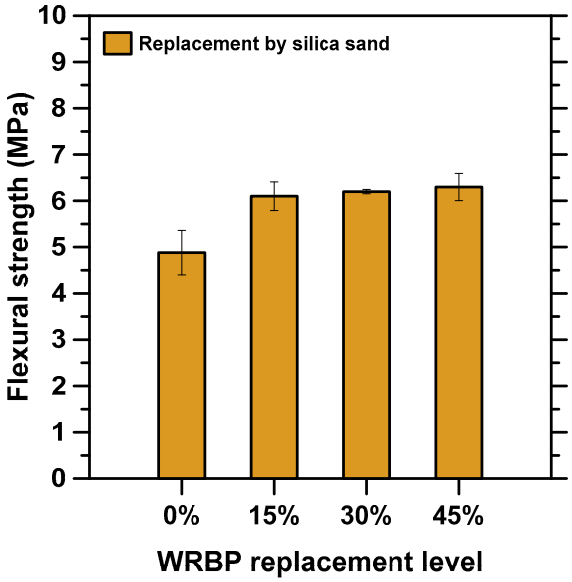

Figure 7. FS of AAMs against varying WRBP contents as silica sand replacement agent.

3.2.3. Effect of Replacement Type (Scenario) on Strength Properties of AAMs

Figure 8 compares the compressive strength development of the AAMs containing WRBP as binder or fine aggregates replacement. It was observed that the use of WRBP as silica sand replacement demonstrated excellent performance compared to that prepared with WRBP as GGBFS and MK replacement. In comparison to the compressive strength of the control specimen devoid of WRBP (37.54 MPa), the compressive strength of the mortars made using 0 to a 15% of WRBP as binder and fine aggregates replacement was increased

from 49.98 to 63.62 MPa, respectively. However, the increasing level of replacement to 30 and 45% led to a change in the compressive strength from 44.82 and 34.2 MPa as binder and 75.80 and 89.62 MPa as fine aggregates. Similar results were obtained for the flexural strength of the AAMs wherein the flexural strength was significantly influenced by the type of replacement (as binder or fine aggregates) and level of replacement (15, 30, and 45%). The specimens containing WRBP as fine aggregates displayed higher flexural strength performance compared to other samples as shown in Figure 9.

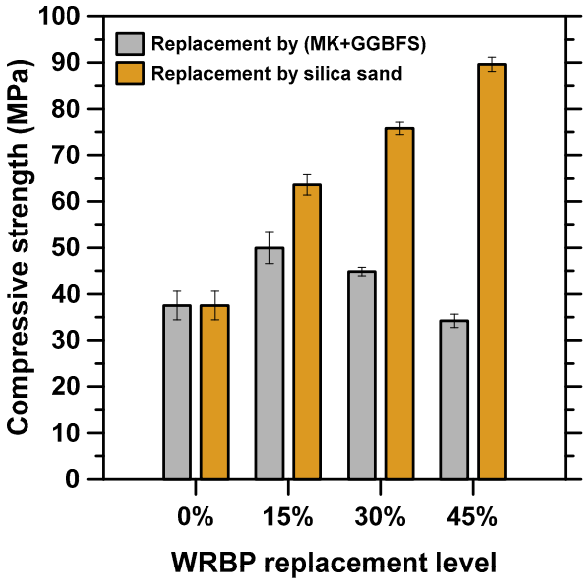

Figure 8. Effect of WRBP replacement type (scenario) on the CS of AAMs cured at ambient temperature for 28 days.

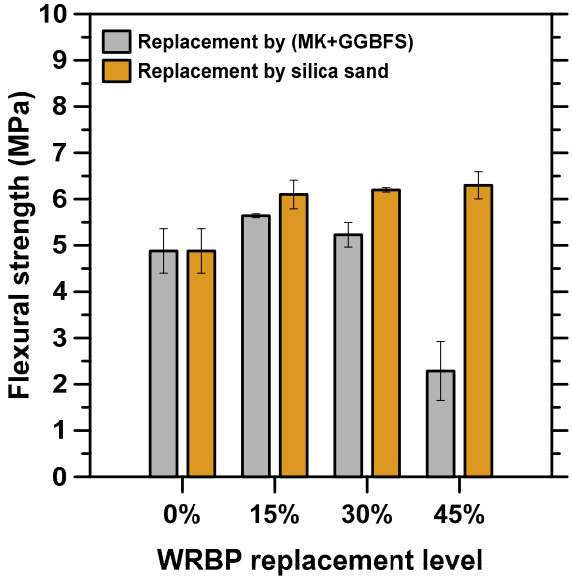

Figure 9. Effect of WRBP replacement type (scenario) on the FS of AAMs cured at ambient temperature for 28 days.

3.2.4. Influence of Curing Temperatures on Strength Properties of AAMs

Figures 10 and 11 display the influence of various curing temperatures on the compressive strength and flexural strength of the studied AAMs prepared with various levels of WRBP as GGBFS and MK replacement, respectively. Specimens were cured at 25, 300, and 600 °C and the average value of tested three specimens for each batch was considered.

As shown in Figure 10, for all the mortar specimens, the compressive strength shows a decreasing trend with increasing curing temperatures. For the control sample (0% of WRBP), the increasing curing temperature from 25 to 600 °C resulted in a drop in compressive strength from 37.54 to 16.92 MPa, respectively. However, the inclusion of 45% WRBP led to a reduction in strength from 35.3 to 25.2% at 300 °C and from 54.9 to 46.7% at 600 °C. A similar trend of results was observed for the flexural strength test, and strength was negatively influenced by increasing the curing temperature from 25 °C to 600 °C. However, replacing GGBFS and MK by WRBP significantly reduced flexural strength under high curing temperatures (Figure 11).

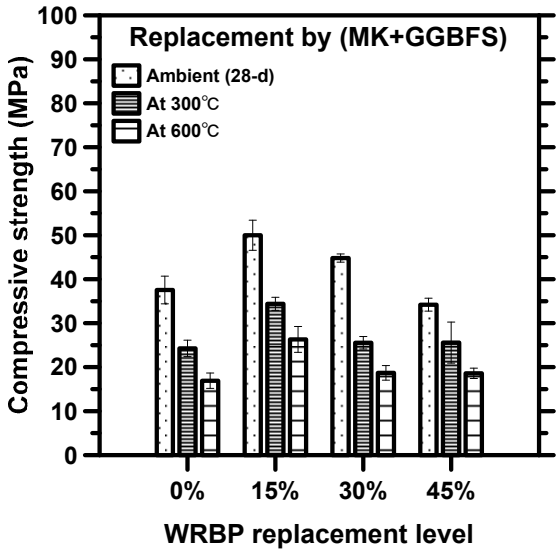

Figure 10. Effects of various curing temperatures on the CS of AAMs made using WRBP replacement by (MK+GGBFS) scenarios.

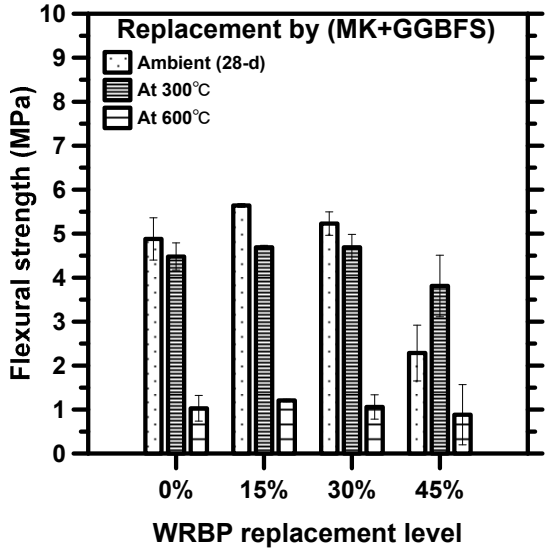

Figure 11. Effects of various curing temperatures on the FS of AAMs made using WRBP replacement by (MK+GGBFS) scenarios.

The observed decrease in the CS of AAMs due to the increase in the curing temperatures to 300 and 600 °C were attributed to the increase in pore structure and internal crack development by the heating process that induced the formation of micro-cracks [38]. Furthermore, as the temperatures were increased to 600 °C, the dense structure was transformed to the progressively less compact structure with a visible network of micro-cracks

and large pores. Abdulkareem et al. [44] found a stabilization in the weight loss rate from 150 °C to 780 °C, which was attributed to the evaporation of both chemically bonded water and hydroxyl groups OH, which negatively affected strength performance.

Figures 12 and 13 show the influence on the compressive strength and flexural strength of the prepared AAMs due to the inclusion of WRBP as silica sand replacement, respectively. It was found that the AAMs containing 0 and 15% of WRBP were significantly influenced by the curing temperatures and the values decreased with the increase in curing temperatures from ambient temperature to 300 and 600 °C. However, the specimens of prepared AAMs containing 30 and 45% of WRBP and cured at 300 °C displayed an enhancement in compressive strength compared to the control sample. Contrarily, the increasing curing temperature to 600 °C led to a drop in compressive strength, being lower than the control sample. Similar results were observed (Figure 13) for the flexural strength; the specimens containing a high amount of WRBP (30 and 45%) that were cured at 300 °C achieved an increment in flexural strength values compared to the control sample. However, all the mortars containing various levels of WRBP (0, 15, 30, and 45%) were influenced by increasing the curing temperature to 600 °C and displayed lower strength compared to the control sample.

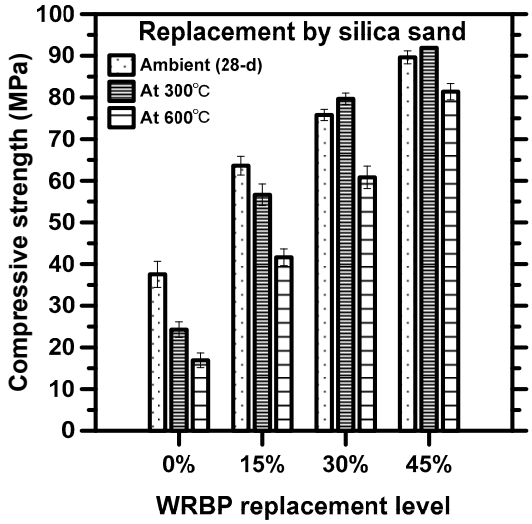

Figure 12. Effect of curing temperatures on the CS of AAMs prepared using WRBP replacement by sand scenarios.

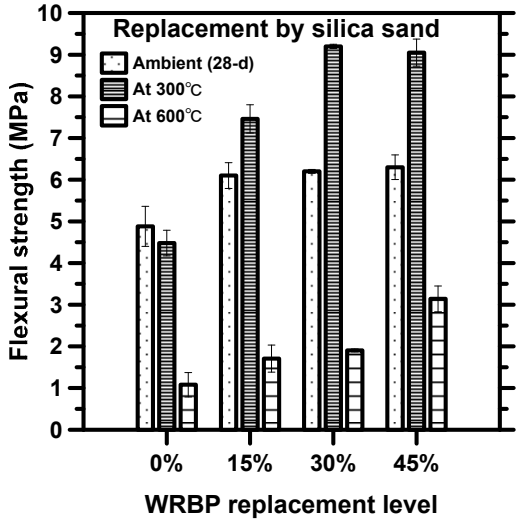

Figure 13. Effect of curing temperatures on the FS of AAMs prepared using WRBP replacement by sand scenarios.

3.2.5. Relationship between Bulk Density and CS of AAMs

Figure 14 displays the relationship between bulk density and compressive strength of prepared mortars with WRBP as binder or fine aggregate replacement that were obtained under different curing temperatures. The specimens containing WRBP as GGBFS and MK replacement and cured at ambient temperature displayed direct relationship between the compressive strength and bulk density. The compressive strength tended to increase with increasing bulk density of prepared specimens. Contrarily, for the specimens cured at 300 and 600 °C, it was found that the compressive strength tended to decrease with increasing bulk density. However, for the specimens containing WRBP as silica sand replacement, the inverse relationship between compressive strength and bulk density was observed, for all different curing regimes (ambient, 300, and 600 °C). It was found that with an increase in bulk density, the compressive strength tended to decrease and displayed lower values.

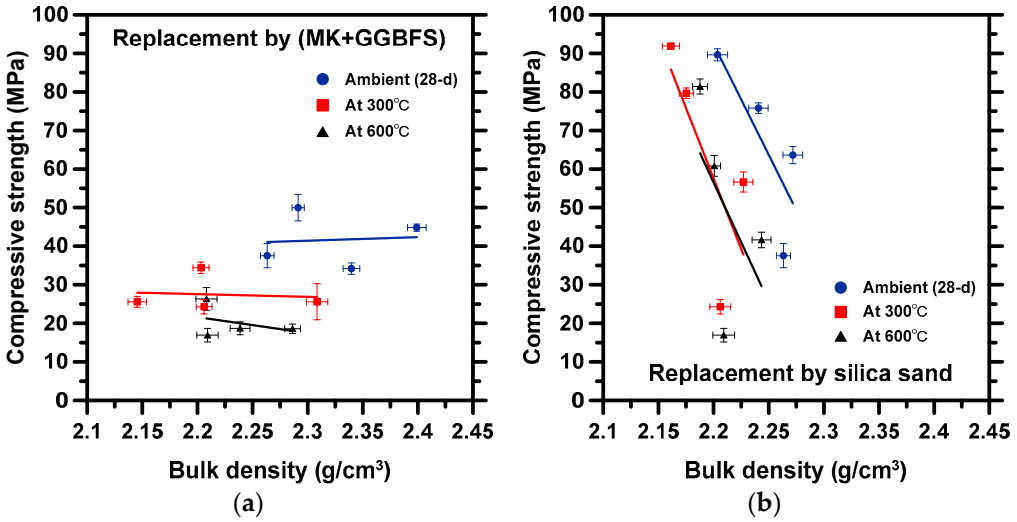

Figure 14. Relationship between CS and bulk densities of AAMs prepared using WRBP replacement by (**a**) (MK+GGBFS) and (**b**) silica sand.

3.3. Chemical Durability and Microstructures Characteristics

3.3.1. Effect of WRBP on Efflorescence and Visual Appearance of Mortars

Figure 15 displays the effect of WRBP as binder or fine aggregates replacement on the efflorescence and visual appearance of alkali-activated mortar specimens. The addition of WRBP in the AAMs could significantly reduce the efflorescence and improve the mortars' durability. The mortar containing 45% of WRBP displayed the optimum performance compared to other specimens. However, the specimen containing 45% of WRBP as GGBFS and MK showed more pores in the surface morphology compared to the control sample.

3.3.2. XRD Analysis

Figure 16 illustrates the XRD pattern of the AAMs containing 0 and 45% of WRBP as silica sand replacement at 28 days of curing age. The intensities of quartz peaks at degree of 21, 28.1, 42.5, 55, 60, and 75 were found to decrease with the increasing content of WRBP from 0 to 45% as silica sand replacement. The reduction in the intensity of quartz peaks with the inclusion of 45% of WRBP can be attributed to the participation of more SiO_2 in the geopolymerization process, formulating more dense gels that contributed to the improvement in CS of the AAMs compared to the control sample. In addition, the XRD pattern of the specimen containing 45% of WRBP showed more amorphous phase compared to the specimen prepared with 0% of WRBP. The lower crystallinity in the AAMs containing 45% of WRBP was responsible for the lower amount of non-reacted particles and significant increment in the N, C-(A)-S-H gels formation.

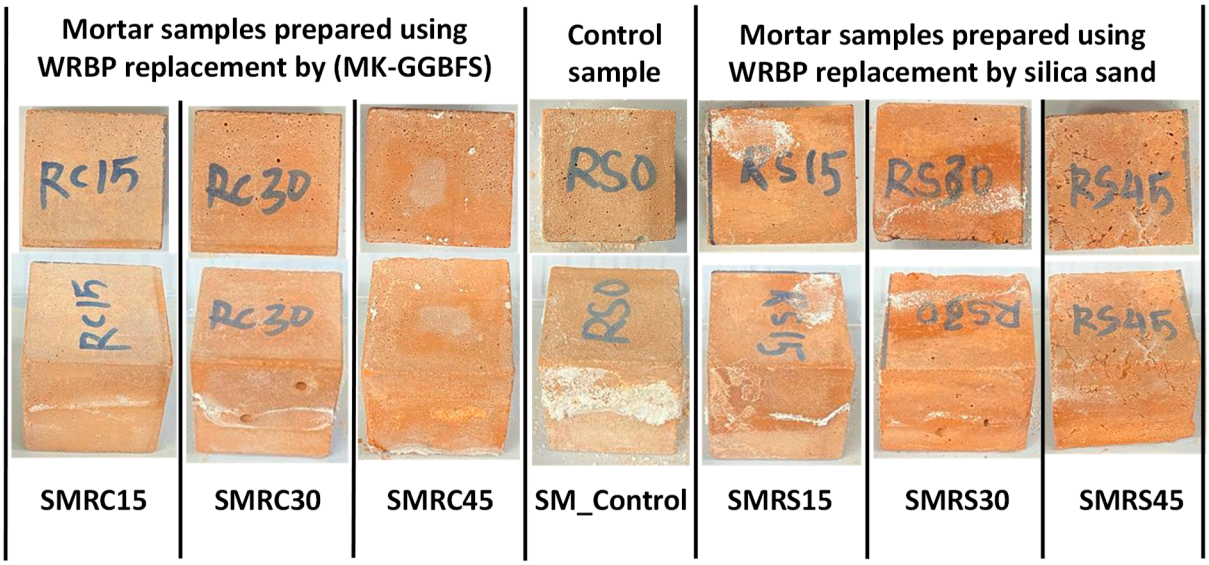

Figure 15. Appearance of efflorescence.

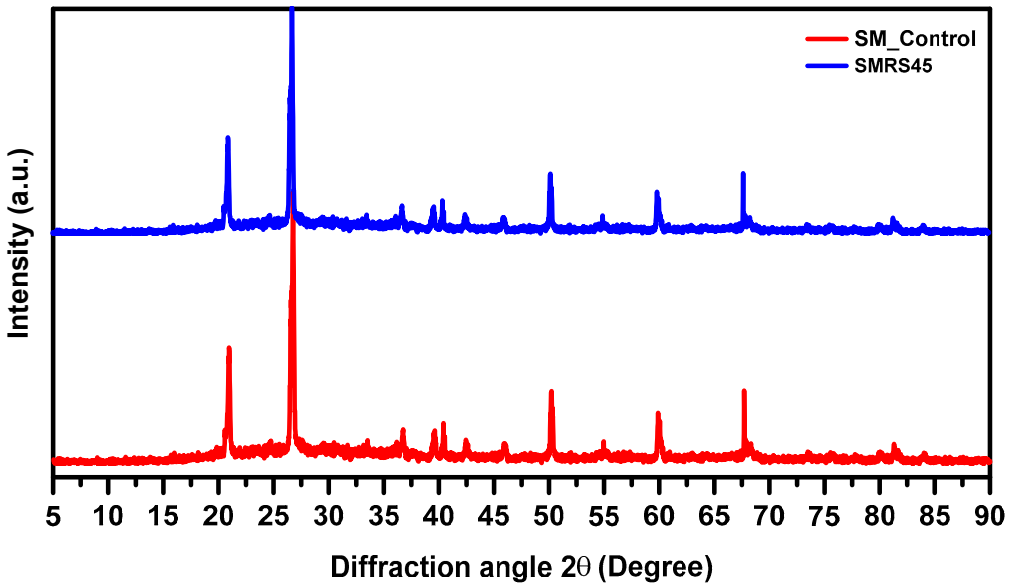

Figure 16. XRD pattern of control and SMRS45 samples.

3.3.3. SEM Images

Figure 17 shows the SEM images of AAMs at 28 days of curing age. The presence of WRBP was found to have considerable effect on the surface morphology of AAMs. The inclusion of 45% of WRBP as silica sand replacement was found to enhance the geopolymerization reaction and increase the dense gels (N, C-(A)-S-H), reducing the total pores (Figure 17b). A comparison of the SEM images of the control specimen (Figure 17a) with those containing 45% of WRBP as silica sand replacement showed a reduction in the numbers of pores and non-reacted particles, leading to the enhancement in the mechanical properties of AAMs.

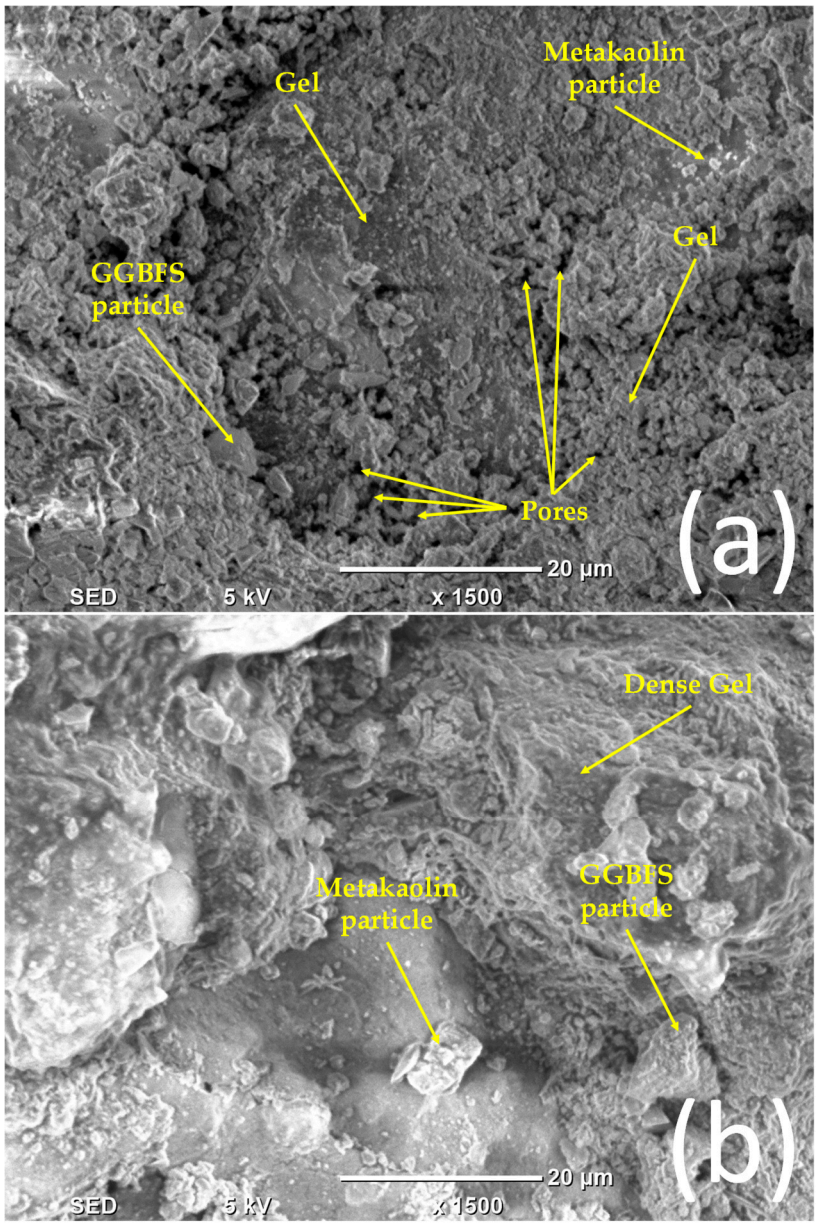

Figure 17. SEM micrographs of (**a**) control (**b**) SMRS45 samples.

4. Conclusions

This study evaluated the effect of WRBP inclusion as binder or fine aggregates replacement on the workability, compressive, flexural strengths, surface morphology, and microstructures of a new type of AAMs prepared for the first time. Based on the obtained results and detail analyses, the following conclusions are drawn:

1. The addition of WRBP in the alkali-activated matrix as binder (GGBFS+MK) or fine aggregates (silica sand) significantly affected the workability performance wherein the flow of the fresh mortar was decreased with the increase in WRBP content.
2. The bulk density of the studied mortars was significantly influenced by the variation in WRBP content and curing regime. The replacement of GGBFS and MK by increasing the level of WRBP from 0 to 45% led to an increase in the bulk density of the mortars. Contrarily, the inclusion of WRBP as silica sand replacement led to a decrease in the bulk density of the prepared specimens. In short, the bulk density of the AAMs was considerably influenced by the curing regime wherein the specimens cured at higher temperature showed lower density.

3. Replacement of GGBFS and MK by 15% of WRBP led to an enhancement in the compressive strength performance of the mortar by 30.7%. However, further increase in the WRBP content up to 45% led to a significant drop in the compressive strength performance of the mortars. Likewise, the flexural strength performance was significantly improved with the inclusion of 15% of WRBP in the AAMs matrix as GGBFS and MK replacement.
4. The incorporation of WRBP as partial replacement of silica sand resulted in a sharp increase in the strength performance of the AAMs.
5. As curing temperature was increased from the ambient temperature to 600 °C, the strength values of the mortars decreased, indicating that the curing regime had a negative impact on the AAMs' strength performance.
6. The addition of WRBP to the mortar matrix significantly reduced the efflorescence on the surface of the proposed AAMs.
7. Microstructural analysis using XRD and SEM showed that adding 45% WRBP to mortars in place of silica sand increased the density of the gels and decreased the pore size. The gained improvement in mortar surface morphology has the potential to significantly improve the strength performance of mortars.
8. Overall, the workability, strengths, surface morphology, and microstructures of the proposed AAMs were appreciably affected by the incorporation of WRBP as binder or fine aggregates substitution.
9. It was concluded that recycling of WRBP in the manufacturing of cement-free (green) AAMs can be beneficial for construction industries in terms of lowering landfill problems and environment issues, thus contributing significantly to the cause of sustainable development.

Author Contributions: Conceptualization, H.A. and A.A.A.; methodology, H.A., A.A.A.; validation, M.K., M.A. and A.A.; formal analysis, H.A. and A.A.A.; investigation, M.A. and A.A.; resources, A.A.A.; data curation, M.K.; writing—original draft preparation, H.A.; writing—review and editing, A.A.A.; visualization, M.A.; supervision, A.A.A. and H.A.; project administration, M.K. and A.A. All authors have read and agreed to the published version of the manuscript.

Funding: The authors extend their appreciation to the Deputyship for Research and Innovation, Ministry of Education in Saudi Arabia for funding this research work through the project no. (IFKSUOR3–383–1).

Data Availability Statement: Not applicable.

Conflicts of Interest: The authors declare no conflict of interest.

References

1. Rakhimova, N.R.; Rakhimov, R.Z. Alkali-activated cements and mortars based on blast furnace slag and red clay brick waste. *Mater. Des.* **2015**, *85*, 324–331. [CrossRef]
2. Huseien, G.F.; Shah, K.W. Durability and life cycle evaluation of self-compacting concrete containing fly ash as GBFS replacement with alkali activation. *Constr. Build. Mater.* **2020**, *235*, 117458. [CrossRef]
3. Huseien, G.F.; Sam, A.R.M.; Algaifi, H.A.; Alyousef, R. Development of a sustainable concrete incorporated with effective microorganism and fly Ash: Characteristics and modeling studies. *Constr. Build. Mater.* **2021**, *285*, 122899. [CrossRef]
4. Kongar-Syuryun, C.; Aleksakhin, A.; Khayrutdinov, A.; Tyulyaeva, Y. Research of rheological characteristics of the mixture as a way to create a new backfill material with specified characteristics. *Mater. Today Proc.* **2021**, *38*, 2052–2054. [CrossRef]
5. Rovnaník, P.; Rovnanikova, P.; Vyšvařil, M.; Grzeszczyk, S.; Janowska-Renkas, E. Rheological properties and microstructure of binary waste red brick powder/metakaolin geopolymer. *Constr. Build. Mater.* **2018**, *188*, 924–933. [CrossRef]
6. Kongar-Syuryun, C.B.; Faradzhov, V.; Tyulyaeva, Y.S.; Khayrutdinov, A. Effect of activating treatment of halite flotation waste in backfill mixture preparation. *Min. Inf. Anal. Bull* **2021**, *1*, 43–57. [CrossRef]
7. Khayrutdinov, A.; Kongar-Syuryun, C.; Kowalik, T.; Faradzhov, V. Improvement of the backfilling characteristics by activation of halite waste for non-waste geotechnology. *IOP Conf. Ser. Mater. Sci. Eng.* **2020**, *867*, 012018. [CrossRef]
8. Rybak, J.M.; Kongar-Syuryun, C.; Tyulyaeva, Y.; Khayrutdinov, A.M.; Akinshin, I. Geomechanical substantiation of parameters of technology for mining salt deposits with a backfill. *Min. Sci.* **2021**, *28*, 19–32. [CrossRef]
9. Huseien, G.F.; Tahir, M.M.; Mirza, J.; Ismail, M.; Shah, K.W.; Asaad, M.A. Effects of POFA replaced with FA on durability properties of GBFS included alkali activated mortars. *Constr. Build. Mater.* **2018**, *175*, 174–186. [CrossRef]

10. Rashad, A.M. A comprehensive overview about the influence of different admixtures and additives on the properties of alkali-activated fly ash. *Mater. Des.* **2014**, *53*, 1005–1025. [CrossRef]
11. Provis, J.L.; Palomo, A.; Shi, C. Advances in understanding alkali-activated materials. *Cem. Concr. Res.* **2015**, *78*, 110–125. [CrossRef]
12. Castel, A.; Foster, S.J. Bond strength between blended slag and Class F fly ash geopolymer concrete with steel reinforcement. *Cem. Concr. Res.* **2015**, *72*, 48–53. [CrossRef]
13. Shekhawat, P.; Sharma, G.; Singh, R.M. Strength behavior of alkaline activated eggshell powder and flyash geopolymer cured at ambient temperature. *Constr. Build. Mater.* **2019**, *223*, 1112–1122. [CrossRef]
14. Samadi, M.; Shah, K.W.; Huseien, G.F.; Lim, N.H.A.S. Influence of Glass Silica Waste Nano Powder on the Mechanical and Microstructure Properties of Alkali-Activated Mortars. *Nanomaterials* **2020**, *10*, 324. [CrossRef] [PubMed]
15. Abadel, A.A.; Alghamdi, H. Effect of high volume tile ceramic wastes on resistance of geopolymer mortars to abrasion and freezing-thawing cycles: Experimental and deep learning modelling. *Ceram. Int.* **2023**, *49*, 15065–15081. [CrossRef]
16. Asaad, M.A.; Huseien, G.F.; Memon, R.P.; Ghoshal, S.; Mohammadhosseini, H.; Alyousef, R. Enduring performance of alkali-activated mortars with metakaolin as granulated blast furnace slag replacement. *Case Stud. Constr. Mater.* **2022**, *16*, e00845. [CrossRef]
17. Du, K.; Xie, C.; Ouyang, X. A comparison of carbon dioxide (CO_2) emission trends among provinces in China. *Renew. Sustain. Energy Rev.* **2017**, *73*, 19–25. [CrossRef]
18. Abdel-Gawwad, H.A.; Rashad, A.M.; Mohammed, M.S.; Tawfik, T.A. The potential application of cement kiln dust-red clay brick waste-silica fume composites as unfired building bricks with outstanding properties and high ability to CO_2-capture. *J. Build. Eng.* **2021**, *42*, 102479. [CrossRef]
19. Sedira, N.; Castro-Gomes, J.; Magrinho, M. Red clay brick and tungsten mining waste-based alkali-activated binder: Microstructural and mechanical properties. *Constr. Build. Mater.* **2018**, *190*, 1034–1048. [CrossRef]
20. Li, H.; Dong, L.; Jiang, Z.; Yang, X.; Yang, Z. Study on utilization of red brick waste powder in the production of cement-based red decorative plaster for walls. *J. Clean. Prod.* **2016**, *133*, 1017–1026. [CrossRef]
21. Reig, L.; Tashima, M.M.; Borrachero, M.; Monzó, J.; Cheeseman, C.; Payá, J. Properties and microstructure of alkali-activated red clay brick waste. *Constr. Build. Mater.* **2013**, *43*, 98–106. [CrossRef]
22. Sudhir, M.; Beulah, M.; Rai, P.S.; Gayathri, G. A microstructure exploration and compressive strength determination of red mud bricks prepared using industrial wastes. *Mater. Today Proc.* **2021**, *46*, 163–169. [CrossRef]
23. Huseien, G.F.; Mirza, J.; Ismail, M.; Ghoshal, S.; Ariffin, M.A.M. Effect of metakaolin replaced granulated blast furnace slag on fresh and early strength properties of geopolymer mortar. *Ain Shams Eng. J.* **2018**, *9*, 1557–1566. [CrossRef]
24. Candamano, S.; De Luca, P.; Frontera, P.; Crea, F. Production of geopolymeric mortars containing forest biomass ash as partial replacement of metakaolin. *Environments* **2017**, *4*, 74. [CrossRef]
25. Medri, V.; Papa, E.; Lizion, J.; Landi, E. Metakaolin-based geopolymer beads: Production methods and characterization. *J. Clean. Prod.* **2020**, *244*, 118844. [CrossRef]
26. Ma, Z.; Tang, Q.; Wu, H.; Xu, J.; Liang, C. Mechanical properties and water absorption of cement composites with various fineness and contents of waste brick powder from C&D waste. *Cem. Concr. Compos.* **2020**, *114*, 103758.
27. Liang, G.; Luo, L.; Yao, W. Reusing waste red brick powder as partial mineral precursor in eco-friendly binders: Reaction kinetics, microstructure and life-cycle assessment. *Resour. Conserv. Recycl.* **2022**, *185*, 106523. [CrossRef]
28. Migunthanna, J.; Rajeev, P.; Sanjayan, J. Waste Clay Bricks as a Geopolymer Binder for Pavement Construction. *Sustainability* **2022**, *14*, 6456. [CrossRef]
29. Fořt, J.; Vejmelková, E.; Koňáková, D.; Alblová, N.; Čáchová, M.; Keppert, M.; Rovnaníková, P.; Černý, R. Application of waste brick powder in alkali activated aluminosilicates: Functional and environmental aspects. *J. Clean. Prod.* **2018**, *194*, 714–725. [CrossRef]
30. Migunthanna, J.; Rajeev, P.; Sanjayan, J. Investigation of waste clay brick as partial replacement of geopolymer binders for rigid pavement application. *Constr. Build. Mater.* **2021**, *305*, 124787. [CrossRef]
31. Huseien, G.F.; Ismail, M.; Khalid, N.H.A.; Hussin, M.W.; Mirza, J. Compressive strength and microstructure of assorted wastes incorporated geopolymer mortars: Effect of solution molarity. *Alex. Eng. J.* **2018**, *57*, 3375–3386. [CrossRef]
32. Cho, Y.-K.; Yoo, S.-W.; Jung, S.-H.; Lee, K.-M.; Kwon, S.-J. Effect of Na_2O content, SiO_2/Na_2O molar ratio, and curing conditions on the compressive strength of FA-based geopolymer. *Constr. Build. Mater.* **2017**, *145*, 253–260. [CrossRef]
33. Dehghani, A.; Aslani, F.; Panah, N.G. Effects of initial SiO_2/Al_2O_3 molar ratio and slag on fly ash-based ambient cured geopolymer properties. *Constr. Build. Mater.* **2021**, *293*, 123527. [CrossRef]
34. *ASTM C33-07*; Standard Specifications for Concrete Aggregates. ASTM: West Conshohocken, PN, USA, 2003.
35. *ASTM C230/C230M-03*; Standard Specification for Flow Table for Use in Tests of Hydraulic Cement. ASTM: West Conshohocken, PA, USA, 2014; pp. 1–6.
36. *ASTM C109*; Standard Test Method for Compressive Strength of Hydraulic Cement Mortars (Using 2-in. or [50-mm] Cube Specimens). ASTM: West Conshohocken, PN, USA, 2012.
37. *ASTM C78/C78M-18*; Standard Test Method for Flexural Strength of Concrete Using Simple Beam with Third-Point Loading. ASTM: West Conshohocken, PN, USA, 2018.

38. Kuri, J.C.; Khan, M.N.N.; Sarker, P.K. Workability, strength and microstructural properties of ground ferronickel slag blended fly ash geopolymer mortar. *J. Sustain. Cem. Based Mater.* **2022**, *11*, 75–87. [CrossRef]
39. Huseien, G.F.; Sam, A.R.M.; Shah, K.W.; Budiea, A.; Mirza, J. Utilizing spend garnets as sand replacement in alkali-activated mortars containing fly ash and GBFS. *Constr. Build. Mater.* **2019**, *225*, 132–145. [CrossRef]
40. Huseien, G.F.; Hamzah, H.K.; Sam, A.R.M.; Khalid, N.H.A.; Shah, K.W.; Deogrescu, D.P.; Mirza, J. Alkali-activated mortars blended with glass bottle waste nano powder: Environmental benefit and sustainability. *J. Clean. Prod.* **2020**, *243*, 118636. [CrossRef]
41. Kubba, Z.; Huseien, G.F.; Sam, A.R.M.; Shah, K.W.; Asaad, M.A.; Ismail, M.; Tahir, M.M.; Mirza, J. Impact of curing temperatures and alkaline activators on compressive strength and porosity of ternary blended geopolymer mortars. *Case Stud. Constr. Mater.* **2018**, *9*, e00205. [CrossRef]
42. Rakhimova, N.; Rakhimov, R. Alkali-activated slag-blended cements with silica supplementary materials. *Inorg. Mater.* **2012**, *48*, 960–964. [CrossRef]
43. Roviello, G.; Ricciotti, L.; Ferone, C.; Colangelo, F.; Tarallo, O. Fire resistant melamine based organic-geopolymer hybrid composites. *Cem. Concr. Compos.* **2015**, *59*, 89–99. [CrossRef]
44. Abdulkareem, O.A.; Al Bakri, A.M.; Kamarudin, H.; Nizar, I.K.; Ala'eddin, A.S. Effects of elevated temperatures on the thermal behavior and mechanical performance of fly ash geopolymer paste, mortar and lightweight concrete. *Constr. Build. Mater.* **2014**, *50*, 377–387. [CrossRef]